


# Serum starvation-based method of ovarian cancer cell dormancy induction and termination *in vitro*

Szymon Rutecki<sup>1,2</sup>, Agnieszka Leśniewska-Bocianowska<sup>1</sup>, Klaudia Chmielewska<sup>1</sup>, Julia Matuszewska<sup>1</sup>, Eryk Naumowicz<sup>3</sup>, Paweł Uruski<sup>4</sup>, Artur Radziemski<sup>4</sup>, Justyna Mikuła-Pietrasik<sup>1</sup>, Andrzej Tykarski<sup>4</sup> and Krzysztof Książek<sup>1,\*</sup> 

<sup>1</sup>Department of Pathophysiology of Ageing and Civilization Diseases, Poznań University of Medical Sciences, Poznań 61-848, Poland

<sup>2</sup>Poznań University of Medical Sciences Doctoral School, Poznań 60-812, Poland

<sup>3</sup>General Surgery Ward, Medical Centre HCP, Poznań 61-485, Poland

<sup>4</sup>Department of Hypertensiology, Poznań University of Medical Sciences, Poznań 61-848, Poland

\*Correspondence address. Department of Pathophysiology of Ageing and Civilization Diseases, Poznań University of Medical Sciences, Długa 1/2 Str., 61-848, Poznań, Poland. Tel: +48-61-854-92-99; Fax: +48 61-854-90-86; E-mail: kksiazek@ump.edu.pl

## Abstract

Awakening and growth reinitiation by dormant cells may contribute to epithelial ovarian cancer (EOC) relapse. The links between these phenomena are loose because of the limited stock of compelling models of EOC dormancy. Here, we show a simple and convenient dormancy research protocol based on serum starvation. This study was conducted on established EOC cell lines A2780, OVCAR-3, and SKOV-3, as well as on primary EOC cells. Cell growth arrest and proliferation were monitored by assessing the Ki67 antigen, PKH26 fluorescence, and cell cycle distribution. In addition, cells were tested for ERK1/2/p38 MAPK activity ratio, apoptosis, and senescence. The study showed that 72-h serum starvation induces G0/G1 growth arrest of a significant fraction of cells, accompanied by reduced Ki67 and ERK1/2/p38 MAPK activity ratio, without signs of apoptosis or cellular senescence. Moreover, providing cells with 72 h of a medium enriched in 5% serum allows the culture to regain its proliferative potential. At the same time, we attempted to induce and terminate dormancy with Mitomycin C addition and withdrawal, which were unsuccessful. In conclusion, serum starvation is a convenient way to reliably induce dormancy in EOC cells, allowing them to be efficiently awakened for further mechanistic research *in vitro*.

**Keywords:** cancer research; dormant cells; ovarian cancer; serum starvation

## Introduction

Epithelial ovarian cancer (EOC) is one of the most frequent and fatal malignancies of the female genital tract [1]. Tumor relapse is one of the greatest clinical challenges for EOC patients. Approximately 70% of disease relapses occur within the first 2 years after primary cytoreduction and first-line chemotherapy [2]. Although numerous scenarios have been developed to treat relapsed disease with secondary cytoreduction or second-line chemotherapy [3], the prognosis is usually poor. Often, it results from the acquired chemoresistance of cancer cells [4]. The mechanisms of EOC relapse are still elusive and somewhat speculative. It is believed that cancer recurrence may be associated with the presence and activity of cancer stem cells [5] and/or with the induction and awakening of so-called dormant cells [6, 7]. Cancer cell dormancy refers to the incidence of disseminated, residual cancer cells that survived the primary treatment and temporarily lost the ability to replicate. Dormant cells can reinitiate proliferation and spread upon their reactivation by specific and still poorly understood environmental stimuli [8]. Nowadays, dormancy is categorized as cellular (cells exit the division cycle), angiogenic (dividing and dying cells are in equilibrium, maintaining inadequate vascularization), and immune mediated (cytotoxicity of immune cells stopping their progression) [6], with the duration of each state ranging from months to decades, depending on the

cancer type and other patient-specific conditions [9]. Typically, dormant cells are growth arrested in the G0/G1 phase of the cell cycle, and quiescence is the most accurate phenomenon for defining the cellular dormancy phenotype [10].

As for the mechanisms determining cellular dormancy initiation, the most plausible explanation seems to be that some stress signals received by cancer cells from the non-permissive tissue microenvironment prevent the cells from resuming proliferation [11]. In experimental settings, models of dormancy initiation include drug-, cell signaling-, biochemistry-, and extracellular matrix-induced phenomena. These models are not universal, and their suitability is strictly connected to specific cancer cell types [9]. In the case of EOC, the dormancy induction and termination methodology is scarce, making the knowledge of the dormant cell's biological and clinical functions in this kind of malignancy very limited. One of the established models utilizes the physical inhibition of OVCAR-5 cell proliferation *in vitro* using a silica-poly(ethylene glycol) (PEG) hydrogel system. Unfortunately, the viability of cells maintained under those conditions deteriorates quickly (after a few days), significantly jeopardizing its usefulness [12]. The second strategy refers to the re-expression of tumor suppressor gene *aplasia Ras homolog member 1 (ARHI)*, which promotes SKOV-3 cell autophagy *in vitro* and the induction of their dormancy in mice xenografts *in vivo* [13]. Last but not the least, there are reports in

Received: September 19, 2023. Revised: October 26, 2023. Accepted: November 1, 2023. Editorial decision: October 27, 2023.

© The Author(s) 2023. Published by Oxford University Press.

This is an Open Access article distributed under the terms of the Creative Commons Attribution-NonCommercial License (<https://creativecommons.org/licenses/by-nc/4.0/>), which permits non-commercial re-use, distribution, and reproduction in any medium, provided the original work is properly cited. For commercial re-use, please contact [journals.permissions@oup.com](mailto:journals.permissions@oup.com)

which dormancy is treated only as a context for other phenomena and thus is neither initiated nor monitored [14].

This narrow range of available tools for identifying and testing EOC cell dormancy limits the ability to assess the actual significance of this process for tumor relapse development. In addition, the lack of convenient, *in vitro* models restricts the study of cell-specific mechanisms of dormant cell formation and awakening and their transformation into proliferating cells. Guided by these insights, we developed a reliable and easy-to-use *in vitro* method for the induction and termination of EOC cell dormancy based on serum starvation. The model has been validated on three established ovarian cancer lines and primary EOC cells. Moreover, we present for comparison a second model based on the action of Mitomycin C (Mit-C), whose usefulness is incomparably lower.

## Materials and methods

### Chemicals and consumables

Unless otherwise stated, all plastics and chemicals were purchased from Nunc (Roskilde, Denmark) and Merck (Darmstadt, Germany).

### Cell cultures

The ovarian cancer cells A2780 (cat. no. 93112519) were obtained from the European Collection of Cell Cultures (Porton Down, Wiltshire, UK). The SKOV-3 cells (cat. no. HTB-77) and OVCAR-3 cells (cat. no. HTB-161) were purchased from the American Type Culture Collection (Rockville, MD, USA). The A2780 and SKOV-3 cells were grown in RPMI-1640 medium (Biowest, Riverside, MO, USA, cat. no. L0501) with L-glutamine (2 mmol/l), penicillin (100 U/ml), streptomycin (100 g/ml) (Merck, cat. no. G6784), and 10% fetal bovine serum (FBS, Biowest, cat. no. S1810). The OVCAR-3 cells were maintained in RPMI-1640 medium with L-glutamine (2 mmol/l), HEPES (10 mmol/l, Merck, cat. no. HO887), sodium pyruvate (1 mmol/l, Merck, cat. no. S8636), glucose (4500 mg/l, Merck, cat. no. G7021), insulin (0.01 mg/ml, Merck, cat. no. I9278), and 20% FBS. The primary EOC cells (pEOC) were isolated from six chemotherapy-naïve patients with high-grade serous ovarian cancer (stage III or IV according to the criteria of the International Federation of Gynecology and Obstetrics) during cytoreductive surgery. The tumors were cut into small fragments of comparable weight and then placed in 0.05% trypsin–0.02% EDTA (Biowest, cat. no. X0930) for 20 min at 37°C with shaking. The cells were propagated in RPMI-1640 medium supplemented with L-glutamine (2 mM) and 20% FBS. Their cancerous nature was verified according to the expression of epithelium-related antigen (MOC-31) and carcinoma antigen 125 (CA125). This study was conducted in accordance with the Declaration of Helsinki, and approved by the Ethics Committee of Poznań University of Medical Sciences (protocol code 539/21; July 24, 2021), and all patients gave their written informed consent.

### Dormancy induction and termination

Cancer cell dormancy was induced by serum starvation using the following protocol. Cells were grown in a standard growth medium to reach ~70% confluency (point A). The cells were not synchronized to mimic the random and asynchronous cell cycle distribution *in vivo*. Afterward, they were carefully washed with phosphate-buffered saline (PBS) and exposed to serum-free medium (SFM) for 24, 48, and 72 h (point B). To terminate dormancy, cells were incubated with a growth medium re-supplemented with 5% exosome-free FBS (Biowest, cat. no. S181M) for 24, 48, and 72 h (point C). Pilot experiments in which the cells were subjected to MTT assays and trypan blue exclusion tests revealed

that the SFM-based protocol of dormancy induction/termination does not affect cell metabolism or viability. In another set of experiments, cells that reached ~70% confluency were forced to enter dormancy by exposure to Mit-C (Tocris Bioscience, Bristol, UK, cat. no. 3258) used at a concentration of 10 µg/ml for 2 h (OVCAR-3, SKOV-3, pEOCs) or 2.5 µg/ml for 1 h (A2780). After the treatment, cells were allowed to recover in the growth medium supplemented with 5% exosome-free FBS for 24, 48, and 72 h.

### Cell proliferation analysis

Expression of Ki67 was quantified in cells fixed with 4% formaldehyde, permeabilized with 0.3% Triton-X 100 (Merck, cat. no. X100) in PBS [at room temperature (RT) for 10 min], and blocked with 1% bovine serum albumin (Merck, cat. no. A3059), 5% goat serum (Merck, cat. no. G9023), and 0.3% Triton-X 100 in PBS at RT for 1 h. Subsequently, the cells were incubated with rabbit mAb against human Ki67 (D3B5, Cell Signaling Technology, Danvers, MA, cat. no. 9129 T), diluted to 1:400 in the blocking buffer at 4°C overnight. Afterward, the cells were incubated with Goat anti-Rabbit IgG (H+L) Cross-Adsorbed Secondary Antibody, Alexa Fluor™ 488 (Invitrogen, Waltham, MA, cat. no. A11008), diluted to 1:500 in PBS, at RT for 1 h. Then, the samples were mounted with a fluoroshield medium with DAPI (Abcam, Cambridge, UK, cat. no. ab104139) and inspected under an Axio Vert.A1 microscope (Carl-Zeiss, Jena, Germany). In each preparation, 200 random cells were evaluated.

Cell proliferation was also tested using a PKH26 Red Fluorescent Cell Linker Mini kit for General Cell Membrane Labeling [15] (Sigma-Aldrich, Darmstadt, Germany, cat. no. MINI26-1KT), according to the manufacturer's instructions. The results of PKH26 fluorescence were quantified under the Axio Vert.A1 microscope in 200 randomly selected cells.

### Proliferation- and stress-related kinase activity measurements

Extracellular signal-regulated kinase 1/2 (ERK1/2) and p38 mitogen-activated protein kinase (p38 MAPK) activities were quantified using InstantOne™ phospho-ERK1/2 ELISA (cat. no. 85-86012-11) and InstantOne™ phospho-p38 MAPK ELISA (cat. no. 85-86022-11), respectively (Invitrogen). The assays were conducted according to the manufacturer's instructions and finally, the ERK1/2/p38 MAPK activity ratios were calculated.

### Cell cycle distribution and apoptosis

Cells were harvested with trypsin–EDTA solution and then fixed with ice-cold 70% ethanol for 1 h. Then, they were washed with PBS and incubated with 0.1 mg/ml RNase (Merck, cat. no. R4875) and 5 mg/ml propidium iodide (Merck, cat. no. P4170) at RT for 30 min. The distribution of cells (10,000) in the cell cycle and the extent of late apoptosis (subG1 fraction) were determined with flow cytometry using an Amnis® CellStream® (Luminex Corporation, Austin, TX). The results were analyzed with ModFit LT™ Version 5 (Verity Software House, Topsham, ME). Early apoptosis was examined using a fluorescent probe, 5,5',6,6'-tetrachloro-1,1',3,3'-tetraethylbenzimidazolylcarbocyanine iodide (JC-1; Cayman Chemical, cat. no. 10009172), that allows one to determine mitochondrial inner membrane potentials ( $\Delta\Psi_m$ ). JC-1 accumulates in the vital mitochondria, generating red fluorescent J-aggregates, while mitochondrial de-energization associated with apoptosis leads to the formation of green fluorescent monomers. A rise in the green/red fluorescence intensity ratio indicates declined  $\Delta\Psi_m$  values. The results of JC-1 fluorescence were quantified under the Axio Vert.A1 microscope and the BioTek Synergy plate reader (Agilent, Santa Clara, CA, USA).

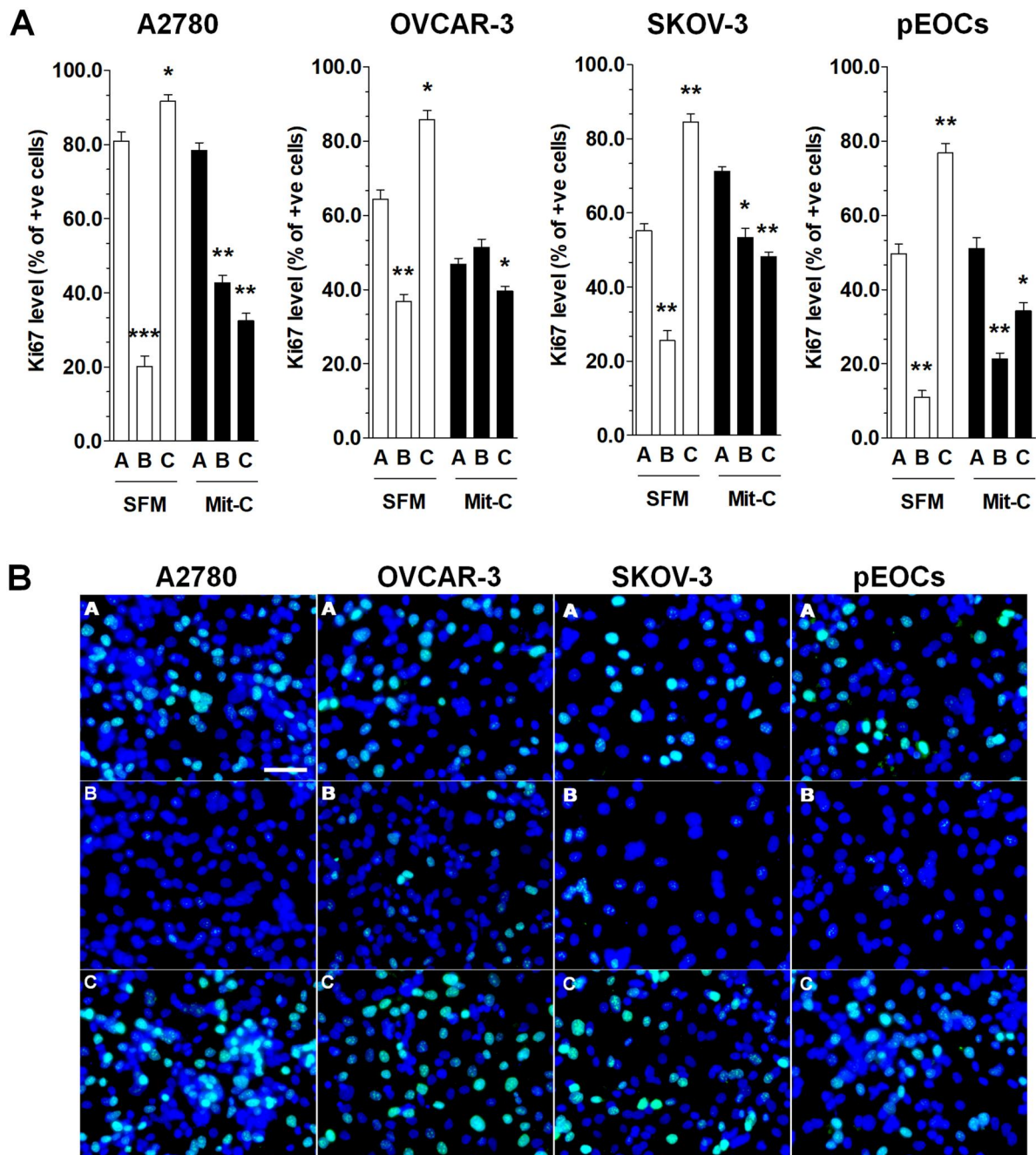


**Figure 1.** Effect of serum starvation (SFM) and Mitomycin C (Mit-C) on the expression of Ki67 in EOC cells. Analysis of the percentage of Ki67-positive cells upon SFM and Mit-C exposure (A). Representative pictures of Ki67 immunofluorescence in serum-starved EOC cells (B). Points A, B, and C refer to the initial (A), dormant (B; 72 h of exposure), and awakened (C; 72 h of exposure) cells. The experiments on established cell lines were performed in hexaplicate, whereas those utilizing pEOCs were conducted on cells from six different donors. The results are expressed as mean  $\pm$  SEM. \* $P < 0.05$ , \*\* $P < 0.01$ , and \*\*\* $P < 0.001$  vs. A. Magnification 400 $\times$ ; scale bar = 500  $\mu$ m.

### Cellular senescence

The senescence of cancer cells was investigated according to the cytosolic activity of senescent-associated  $\beta$ -galactosidase (SA- $\beta$ -Gal). The procedure was performed as described in Sosinska et al. [16] and 200 randomly selected cells were quantified. Briefly, cells were cultured on Lab-Tek™ Chamber Slides (Nunc, Roskilde, Denmark, cat. no. 177445PK), fixed with 3% formaldehyde (Merck, cat. no. F1635), rinsed and exposed for 2 h at 37°C to a solution containing 1 mg/ml 5-bromo-4-chloro-3-indolyl- $\beta$ -D-galactopyranoside (X-Gal, Merck, cat. no. B4252), 5 mM potassium ferrocyanide (Merck, cat. no. P3289), 5 mM potassium ferricyanide (Merck, cat.

no. P8131), 150 mM NaCl (Chempur, Piekary Śląskie, Poland, cat. no. 117941206), 2 mM MgCl<sub>2</sub> (Merck, cat. no. M2393), and 40 mM citric acid (Chempur, cat. no. 115382101) with a pH of 6.0. Cells characterized by the presence of a green precipitant within the cytoplasm were considered positive.

### Statistics

Statistical analysis was performed using GraphPad Prism™ v.6.00 (GraphPad Software, San Diego, CA). The means were compared with repeated ANOVA and a *post hoc* Newman-Keuls test.

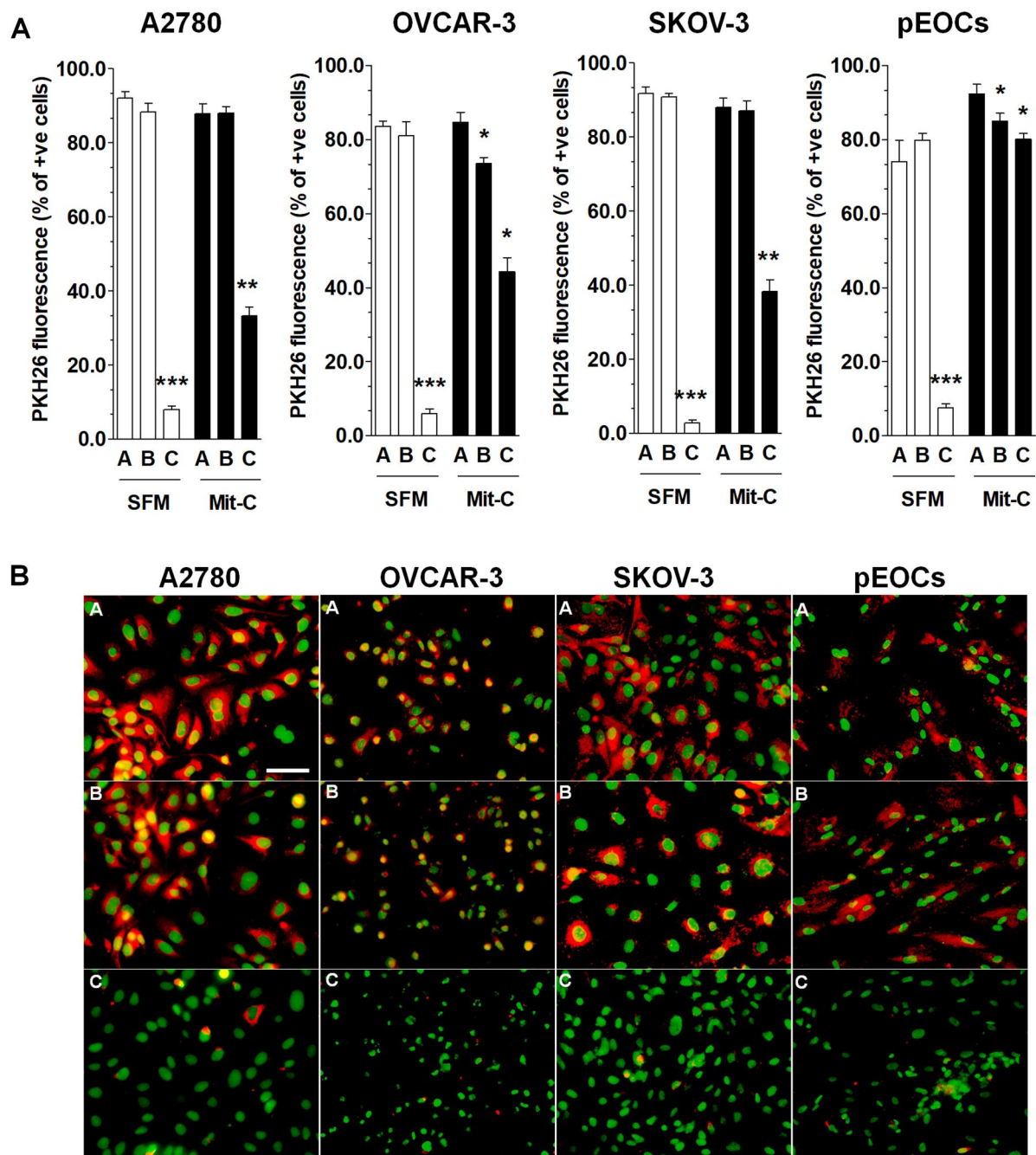


**Figure 2.** Effect of serum starvation (SFM) and Mitomycin C (Mit-C) on PKH26 fluorescence as a measure of EOC cell proliferation. Analysis of the percentage of PKH26-positive cells upon SFM and Mit-C exposure (A). Representative pictures of PKH26 fluorescence in serum-starved EOC cells (B). Points A, B, and C refer to the initial (A), dormant (B; 72 h of exposure), and awakened (C; 72 h of exposure) cells. The experiments on established cell lines were performed in hexaplicate, whereas those utilizing pEOCs were conducted on cells from six different donors. The results are expressed as mean  $\pm$  SEM. \* $P < 0.05$ , \*\* $P < 0.01$ , and \*\*\* $P < 0.001$  vs. A. Magnification 400 $\times$ ; scale bar = 500  $\mu$ m.

The data are shown as the means  $\pm$  SEM. Statistical significance was recognized when the  $P$ -value was less than 0.05.

## Results

### The proliferation of cancer cells subjected to serum deprivation and Mitomycin C

The expression of Ki67 proliferative antigen was quantified using a fluorescence method to examine a decline in ovarian cancer cell proliferation after exposure to SFM and Mit-C. When

asynchronously growing cells (point A) were serum starved for 24 or 48 h, there was no significant reduction in their growth capabilities (not shown). However, when the incubation was extended to 72 h, the fraction of Ki67-positive nuclei decreased remarkably (Fig. 1, point B). Afterward, the cells were subjected to a standard growth medium re-supplemented with 5% exosome-free FBS to recover. The proliferative status of cells did not change during 24 or 48 h (not shown). When the recovery lasted 72 h, cells reinitiated growth as the percentage of Ki67-positive cells dynamically increased and reached higher levels than those representing the

initial cultures (point A) in all cancer cell lines tested (Fig. 1, point C). Higher FBS concentrations at the dormant cell awakening stage were not tested to avoid traumatizing cells.

The proliferation assessment based on the Ki67 level was verified using the fluorescent probe PKH26. The tracer incorporates into cells and spreads to their progeny, which leads to the gradual fading of its fluorescence in proportion to the proliferation rate [15]. The PKH26-related fluorescence in all cancer cell lines tested at point B was comparable to point A, suggesting that serum-deprived cells ceased their proliferation. In contrast, at point C, when a growth medium with 5% FBS was delivered for 72 h, the PKH26 fluorescence significantly declined, confirming that cells recovered and resumed dividing (Fig. 2).

Parallel experiments with cells subjected to Mit-C were performed using a different protocol, including a wide range of concentrations and exposure times. Finally, because of the clearly cytotoxic activity of Mit-C toward all ovarian cancer cells tested, two dosage algorithms were applied, depending on the cancer cell line. Under these conditions, the drug inhibited the proliferation of three out of four cell lines (except OVCAR-3). However, when the cells were induced to recover, the procedure succeeded only in pEOCs. Notably, the fraction of Ki67-positive cells did not return to the level of point A, suggesting only partial recovery (Fig. 1). A2780 and SKOV-3 cells exposed to Mit-C behaved regarding PKH26 fluorescence similarly to their counterparts treated with SFM; however, the decreased fluorescence at point C was evidently lower. In the case of OVCAR-3 cells, the cells recorded at point B had lower fluorescence than at point A, suggesting an ongoing proliferation. The same happened in pEOCs where PKH26 fluorescence at points B and C were lower than cells at point A. Noteworthy, the decrease in fluorescence at point C was not as spectacular as in the case of SFM, which means that the resumption of proliferation after the growth arrest period was relatively small (Fig. 2).

### Cell cycle distribution of cancer cells subjected to serum deprivation and Mitomycin C

Cancer cell distribution in particular cell cycle phases was used as an additional measure of their proliferative status upon serum starvation and Mit-C exposure. As per cells exposed to SFM, all four cancer cell types studied at point B were growth arrested in the G1/G0 phase, which coincided with a decreased fraction of cells in the S phase, that is, those actively replicating DNA. When the starvation ended, and a growth medium with 5% FBS was delivered (point C), the percentage of cells in the S phase considerably increased (Table 1 and Fig. 3).

As per cultures treated with Mit-C, the G1/G0 growth arrest at point B was found only in A2780 cells, and it was accompanied by a decreased S phase. OVCAR-3 cells did not display any changes in cell cycle distribution. SKOV-3 cells became growth arrested at point B in the G2/M phase, which coincided with a decreased S phase. pEOCs also had a reduced fraction of cells in the S phase at point B; however, the exact moment of their growth arrest was not established (Table 1 and Fig. 3).

### Apoptosis and senescence indices in cancer cells subjected to serum deprivation and Mitomycin C

Early apoptosis was determined using JC-1 fluorescence. The analysis showed that either serum-starved cells (point B) or their awakened counterparts (point C) did not display declined  $\Delta\Psi_m$  values, which might indicate an initiation of programmed cell death (Fig. 4). Flow cytometry quantification of cells in the subG1 phase of the cell cycle, that is those bearing low-molecular

**Table 1.** The quantification of ovarian cancer cell cycle distribution under serum deprivation (SFM) and Mitomycin C (Mit-C) exposure.

A2780	SFM			Mit-C		
	G1/G0	S	G2/M	G1/G0	S	G2/M
A	40±2	41±2	19±2	36±1	44±1	20±1
B	56±2*	22±1**	22±2	71±2**	10±4***	19±4
C	53±4	43±3##	4±1	63±2	9±2	28±2
OVCAR-3	SFM			Mit-C		
	G1/G0	S	G2/M	G1/G0	S	G2/M
A	40±2	45±1	15±2	56±2	40±2	4±2
B	51±1*	28±2**	21±1	54±1	40±2	6±2
C	45±1	48±1###	7±1	50±1	35±2	15±2
SKOV-3	SFM			Mit-C		
	G1/G0	S	G2/M	G1/G0	S	G2/M
A	39±5	56±7	5±3	75±1	22±1	3±1
B	73±1*	26±1**	1±1	74±1	13±1**	13±1**
C	30±2####	70±2####	0±0	63±2	27±2###	10±0
pEOCs	SFM			Mit-C		
	G1/G0	S	G2/M	G1/G0	S	G2/M
A	39±3	52±3	9±3	70±2	23±2	7±1
B	57±2**	23±1**	20±2	78±2	14±1**	8±1
C	26±1##	72±1###	2±0	53±2##	37±4####	10±2

Time points A, B, and C correspond to the three stages of the experiment, that is, baseline, dormancy induction, and awakening of dormant cells.

Experiments performed on established cell lines were done using six experimental replicates, whereas experiments on pEOCs were conducted on cultures obtained from six different patients. Results are expressed as mean ± SEM.

- \*  $P < 0.05$ ,
- \*\*  $P < 0.01$  vs. A,
- \*\*\*  $P < 0.001$  vs. A,
- ##  $P < 0.01$  vs. B,
- ###  $P < 0.001$  vs. B.

weight and fragmented DNA, was performed, in turn, to investigate the extent of late apoptosis. As shown in Fig. 5, serum-starved A2780 and OVCAR-3 cells displayed an increased fraction of apoptotic cells, but the magnitude of death was low and did not exceed 10% at points B and C. In SKOV-3 cells, SFM induced more pronounced apoptosis, which reached approximately 30% of cells. Interestingly, when they recovered (point C), the magnitude of apoptosis declined below 3% and was even lower than at point A. Finally, in the case of pEOCs, serum starvation did not change the extent of apoptosis.

Regarding Mit-C exposure, this approach decreased the  $\Delta\Psi_m$  values in A2780, OVCAR-3, and pEOCs cells at either point B or C, whereas in SKOV-3 cells, the  $\Delta\Psi_m$  values remained unchanged (Fig. 4). As per late apoptosis, Mit-C induced it in A2780 cells at point B and the magnitude of this phenomenon at point C was even higher. In OVCAR-3 cells, the percentage of the subG1 cells at points B and C increased compared with point A; however, the recovery did not provoke any additional increase. SKOV-3 cells exposed to Mit-C did not display an elevation of apoptotic cells at point B or C. Finally, pEOCs treated with Mit-C did not experience increased apoptosis at point B; however, the fraction of subG1 cells at point C increased up to 30% (Fig. 5).

The incidence of cellular senescence in serum-starved and Mit-C-treated cells was evaluated according to an expression of SA- $\beta$ -Gal. Cytochemical analysis of this enzyme showed that neither SFM nor Mit-C significantly increased the fraction of

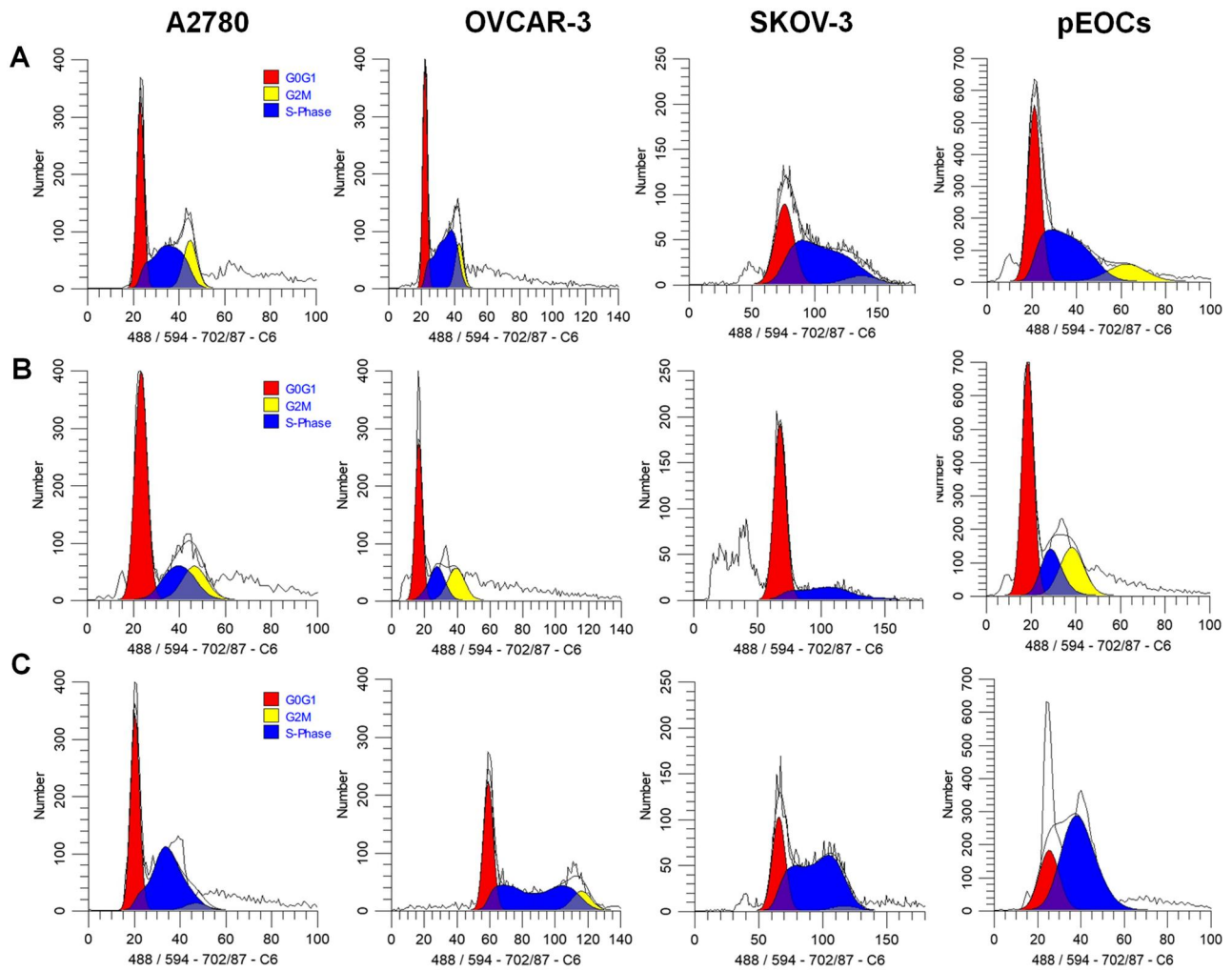


**Figure 3.** Flow cytometry analysis of EOC cell cycle distribution upon serum starvation. Points A, B, and C refer to the initial (A), dormant (B; 72 h of exposure), and awakened (C; 72 h of exposure) cells. A quantitative analysis of histograms, including those for cells treated with Mit-C, is shown in Table 1. The experiments on established cell lines were performed in hexaplicate, whereas those utilizing pEOCs were conducted on cells from six different donors.

senescent cells at points B or C. It should be stressed that the percentage of senescent cells in all cell types and experimental groups investigated did not exceed 2% (Fig. 6).

### Determination of ERK1/2 and p38 MAPK activity

The final verification of the induction and termination of the dormancy state was performed according to an evaluation of the ERK1/2/p38 MAPK activity ratio. This analysis was conducted exclusively using the SFM-based protocol as the only effective method. The quantification of ERK1/2 and p38 MAPK phosphorylation ratios showed that at the initial stage (point A), the activity of ERK1 was markedly higher than the activity of p38 MAPK, yielding a ratio above 1. Conversely, upon serum withdrawal (point B), the situation changed because the activity of p38 MAPK exceeded that of ERK1, generating a ratio below 1. Eventually, when the serum was administered again to reinitiate cell growth (point C), the activity of ERK1/2 increased again, accompanied by decreased activity of p38 MAPK. At this point, the ratio of the two kinases returned to values below 1. This effect was clear and uniform in all cancer cell lines tested (Fig. 7).

## Discussion

Cancer dormancy is still an intriguing but conceptually challenging phenomenon [17]. No one knows the dormant cells' exact origin and molecular characteristics *in vivo*, assuming they exist. At the same time, their relevance for cancer relapse resembles the 'Catch 22' paradox. Until the dormant cell wakes up in the patient and the disease relapses, there is no proof that it was dormant. In basic research, dormancy may only be mimicked and artificially induced without evidence of the similarity of experimentally generated dormant cells to their naturally occurring, relapse-producing counterparts. These circumstances stay in sharp opposition to an urgent need to understand and solve the problem of EOC relapse, which may potentially depend on dormant cell emergence and awakening. Unfortunately, the existing methodology [12, 13] does not support investigations of EOC dormancy, especially *in vitro* when triggers and underlying signaling pathways of dormant cell awakening should be mechanistically determined.

The report presented here originates from our attempts to create a protocol for EOC cell dormancy based on published instructions to use it in our experiments focused on environmental

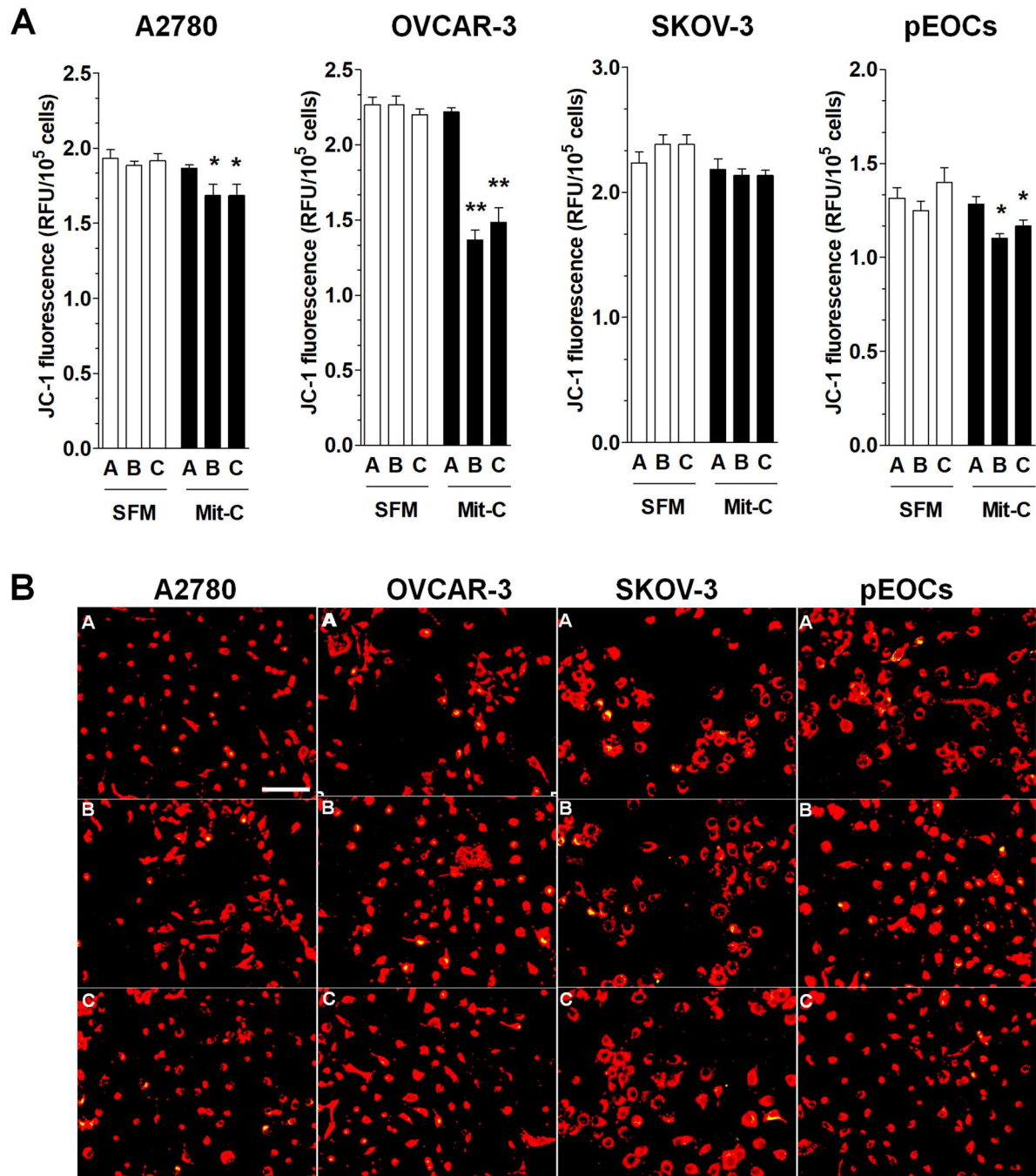


**Figure 4.** Effect of serum starvation (SFM) and Mitomycin C (Mit-C) on the incidence of EOC cell early apoptosis. Quantification of JC-1 fluorescence upon SFM and Mit-C exposure (A). Representative pictures of JC-1 fluorescence in serum-starved EOC cells (B). Red fluorescence indicates J-aggregates, while the yellow (merged) fluorescence indicates that the shift from the red aggregates to green monomers (declined  $\Delta\Psi_m$ ) occurred. Points A, B, and C refer to the initial (A), dormant (B; 72 h of exposure), and awakened (C; 72 h of exposure) cells. The experiments on established cell lines were performed in hexaplicate, whereas those utilizing pEOCs were conducted on cells from six different donors. The results are expressed as mean  $\pm$  SEM. \* $P < 0.05$ ; \*\* $P < 0.01$  vs. A. Magnification 100 $\times$ ; scale bar = 200  $\mu$ m.

triggers of dormant cell development and awakening and potential molecular manipulations that may modulate dormant cell behavior. In fact, it is still unclear whether dormant cells should be treated and if so, what strategy should be employed. In this regard, two scenarios are proposed: eradicating dormant cells using conventional and/or targeted therapies or permanently keeping cells in dormancy, eliminating their ability to wake up [17].

Because literature data clearly show that protocols of dormancy induction are cell type-specific, and those designated for EOC are not fully effective [12], we tried to establish a new, original protocol utilizing Mit-C, a drug successfully used to create cellular feeder layers due to its ability to generate covalent cross-links between DNA opposite strands [18]. Unfortunately, our attempts failed because it has not been possible to obtain a uniform protocol that would allow cells to temporarily stop dividing

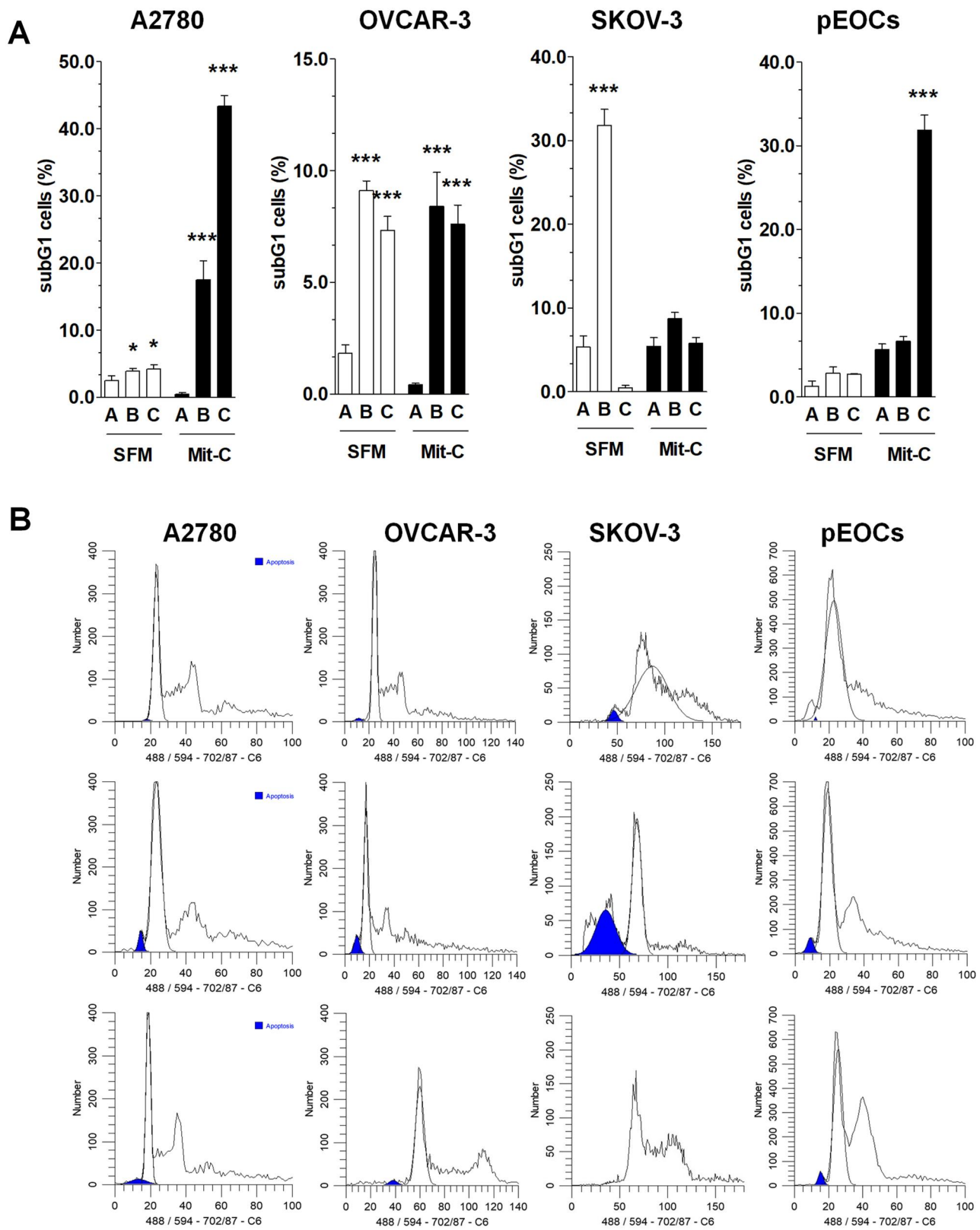


**Figure 5.** Effect of serum starvation (SFM) and Mitomycin C (Mit-C) on the incidence of EOC cell late apoptosis. Analysis of the percentage of apoptotic (subG1) cells upon SFM and Mit-C exposure (A). Representative histograms showing the magnitude of apoptosis in serum-starved EOC cells (B). Points A, B, and C refer to the initial (A), dormant (B; 72 h of exposure), and awakened (C; 72 h of exposure) cells. The experiments on established cell lines were performed in hexaplicate, whereas those utilizing pEOCs were conducted on cells from six different donors. The results are expressed as mean  $\pm$  SEM. \* $P < 0.05$  and \*\*\* $P < 0.001$  vs. A.



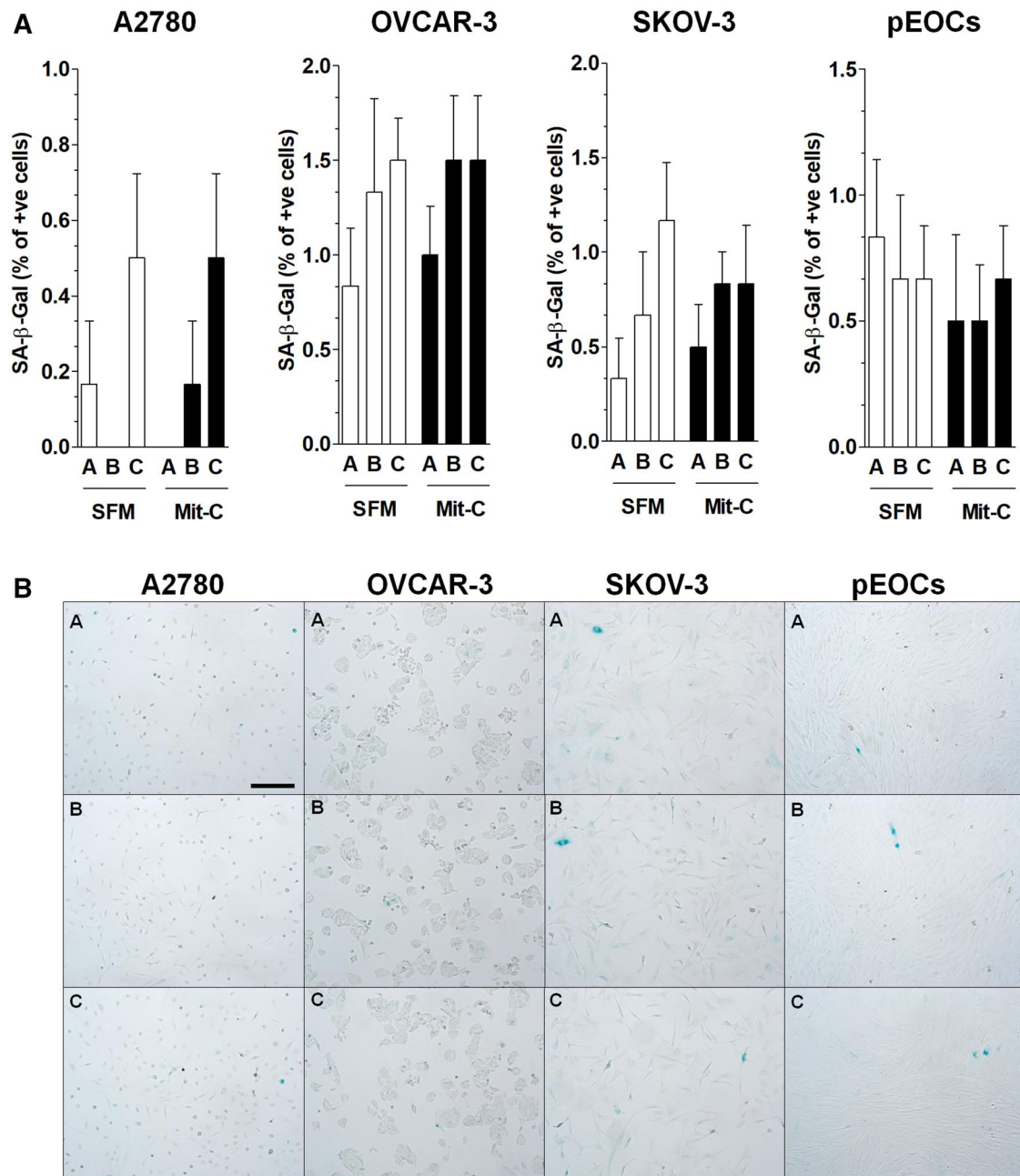


**Figure 6.** Effect of serum starvation (SFM) and Mitomycin C (Mit-C) on cellular senescence occurrence in EOC cells. Analysis of the percentage of senescent (SA-β-Gal-positive) cells upon SFM and Mit-C exposure (A). Representative pictures of SA-β-Gal staining (green cytoplasm) in serum-starved EOC cells (B). Points A, B, and C refer to the initial (A), dormant (B; 72 h of exposure), and awakened (C; 72 h of exposure) cells. The experiments on established cell lines were performed in hexaplicate, whereas those utilizing pEOCs were conducted on cells from six different donors. The results are expressed as mean  $\pm$  SEM. Magnification 100 $\times$ ; scale bar = 200  $\mu$ m.

in the G0/G1 phase and then regain their proliferative activity. These findings are consistent with observations from studies on fibroblasts, which differed significantly in their sensitivity to the anti-proliferative effects of Mit-C [18].

Finally, we employed serum starvation as the driver of EOC dormancy, based on the high nutrient demands of cancer cells that may not be satisfied *in vivo* due to inadequate blood flow through functionally and structurally malformed vessels [19]. In the case of residual cells that survived chemotherapy, their nutrient deficiency may be even more pronounced. This strategy also fits the role of starvation as a determinant of cancer metastasis via translational reprogramming [20]. Last but not least,

nutrient deficiency belongs to a group of postulated extrinsic inducers of dormancy [17] and serum deprivation is a well-known trigger of quiescence [21], treated as the most plausible form of cellular dormancy. Taking the above-mentioned findings into account and based on the research performed, we propose a simple and reliable protocol to induce and terminate dormancy in EOCs triggered by a temporary serum withdrawal (Fig. 8).

The versatility of this method confirmed consistent and reproducible results obtained using primary EOC cell cultures (high-grade serous histotype) and three established cell lines (A2780, OVCAR-3, and SKOV-3) differing in their genetic signatures (including P53 status), histological origin (endometrioid, clear cell,

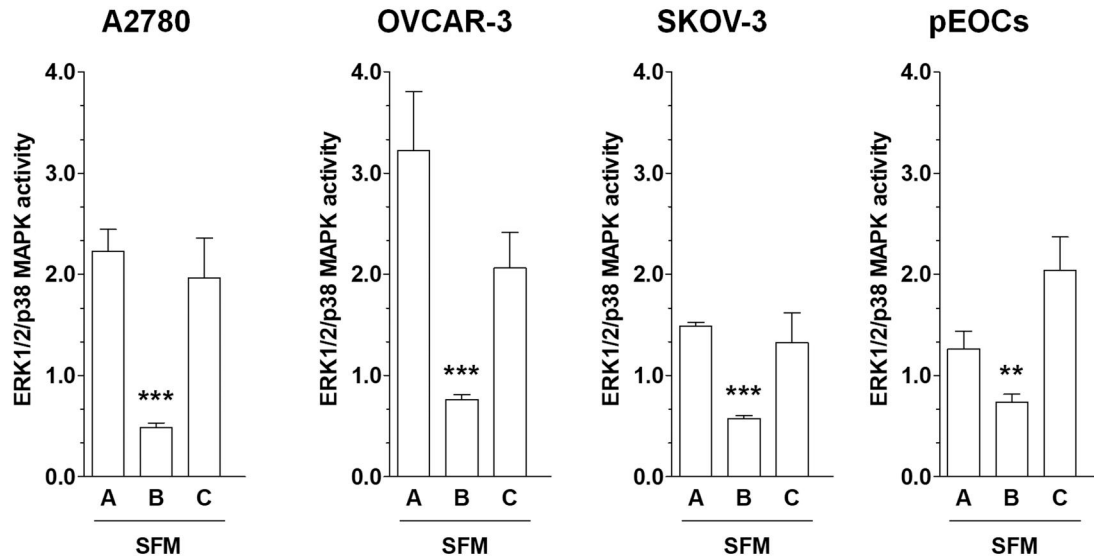


**Figure 7.** Effect of serum starvation (SFM) on ERK1/2/p38 MAPK activity ratio in EOC cells. Points A, B, and C refer to the initial (A), dormant (B; 72 h of exposure), and awakened (C; 72 h of exposure) cells. The experiments on established cell lines were performed in triplicate, whereas those utilizing pEOCs were conducted on cells from four different donors in duplicates. The results are expressed as mean ± SEM. \*\*\*P < 0.001 vs. A.

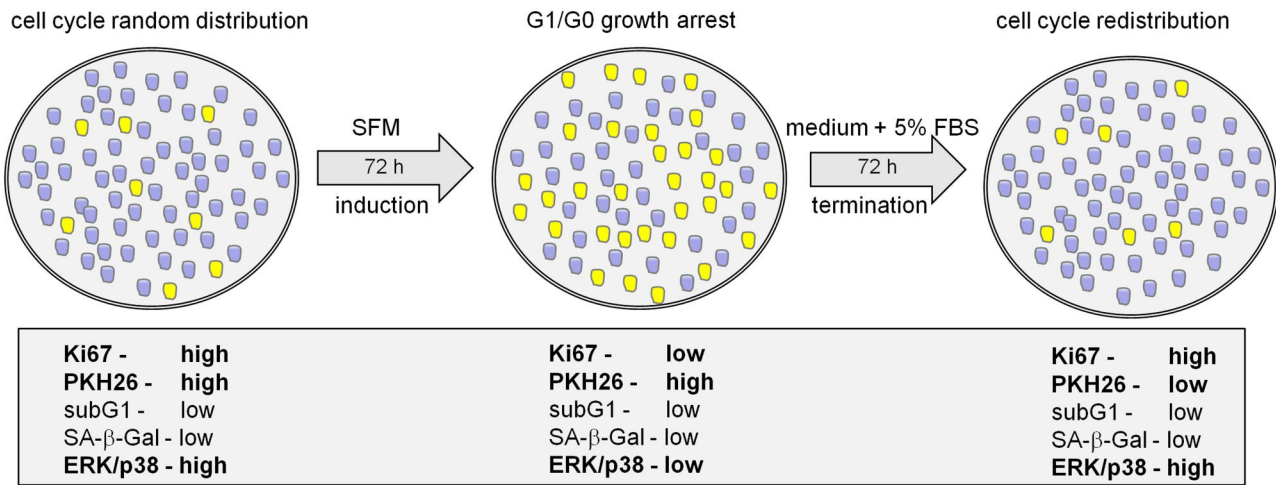


**Figure 8.** A scheme illustrating the established protocol for inducing EOC cell dormancy using serum starvation and dormant cell awakening with 5% FBS re-supplementation. Critical markers distinguishing particular phases of the protocol are shown in bold.

high-grade serous), and aggressiveness [22, 23]. The methodology is based on 3-day serum starvation, which puts a significant subset of cells in quiescence, a sign of cellular dormancy. Recently, elegant proofs for a complex system of serum starvation-dependent cell entry into quiescence were demonstrated on various normal cell types, including human mesenchymal stromal cells [24], fibroblasts, and epithelial cells [25]. In addition, research on prostate cancer cells revealed that serum deprivation initiates their adaptation to oxidative stress acting as a pro-survival stressor [26], which is in line with the general conception of the high resistance of dormant cells to unfavorable chemotherapy-dictated tissue microenvironments [8, 27].

In our model, the dormancy state can be successfully ended by providing 5% exosome-free serum in a standard growth medium for 3 days. The susceptibility of dormant cells to awakening was because 3-day serum starvation put the cells in a state of ‘shallow’ dormancy/quiescence. This conclusion is based on observations of the behavior of serum-starved fibroblasts, whose

ability and dynamics to emerge from the quiescence state depended on the length of their incubation without serum [21].

Phenotypically, serum-starved, dormant ovarian cancer cells display the G1/G0 growth arrest, accompanied by a down-regulated expression of Ki67, a proliferation marker [28]. Because Ki67 is rarely expressed in the G0 phase [29] and abundant in proliferating (S phase) cells with a peak in G2 and early M stages [30], the proliferative status of dormant cells, being a measure of the effectiveness of dormancy induction and termination, was positively verified using a cell phase-independent fluorescent tracer, PKH26 [15].

A separate piece of evidence for the value of the proposed protocol is that the dormant and awakened cells were generally not characterized by a significant increase in the frequency of early or late apoptosis, a phenomenon triggered in some serum-starved cells [31]. At the same time, the stimuli did not activate the senescence program, confirming previous observations pointing that quiescence, associated with inactive TOR, makes

the cells senescence resistant [25]. However, it should also be stressed that the non-proliferative nature of senescent cells sometimes causes them to be equated with dormant cells [8]. This theory, which failed here in the case of ovarian cancer cells, may fit the biology of other cells, for example prostate cancer cells. In their case, bone morphogenetic protein 7 and secreted protein acidic and rich in cysteine maintained dormancy by eliciting senescence [32, 33]. The exclusion of serum starvation-dependent induction of senescence in our model of dormancy induction was also important due to the fact that despite senescence being considered an irreversible exit from the mitotic cycle, it was estimated that one in a million senescent cells could escape from this state and regain the capacity to self-replicate [34].

Another interesting aspect of cancer biology is the mechanisms and signaling pathways behind dormancy induction and termination. Till now, several cellular/molecular events have been recognized to play a role, albeit in this case, their contribution seems to be strictly connected with a particular cell type. These include abnormal signaling derived from  $\beta$ 1-integrins and epidermal growth factor (breast cancer cells [35]), inhibition of AKT combined with increased p130 and p27 (ascites-derived ovarian cancer cells [36]), downregulation of urokinase receptor involving loss of integrin function and MAPK signaling (human squamous carcinoma [37]), ARHI-dependent induction of autophagy (ovarian cancer cells [13]), and many others [17]. Special attention was recently paid to a pair of kinases, ERK1/2 and p38 MAPK, whose reciprocal interactions may both participate in the dormancy status and serve as a marker of this state. In brief, in the course of ERK-dependent proliferation, a high level of p38 MAPK acts as an inhibitor of ERK, preventing cell divisions by triggering the G0–G1 growth arrest, senescence, or apoptosis [38–40]. A luciferase reporter system visualizing the *in vivo* activities of these kinases has shown that dormant cells (breast cancer, prostate cancer, melanoma, and fibrosarcoma) are characterized by increased activity of p38 MAPK and decreased activity of ERK1/2 [38]. Our research performed on a diversified spectrum of ovarian cancer cells confirmed these findings because the proliferating and awakened cells had ERK1/2<sup>HIGH</sup>/p38 MAPK<sup>LOW</sup> phenotypes, whereas their dormant counterparts displayed an inverse activity ratio of both proteins.

Last but not least, it must be stressed that even short-term serum deprivation may initialize other cellular phenomena that have not been experimentally addressed in this study. For example, it may promote endoplasmic reticulum (ER) stress and an unfolded protein response (UPR), both involved in maintaining cellular proteostasis. The activation of ER stress and UPR is particularly important in cancer cells as it determines their progression under non-optimal environmental conditions, by regulating the pro-survival and pro-death equilibrium [41]. Another aspect of serum starvation is the modulation of the mammalian target of rapamycin (mTOR) kinase activity. mTOR is another pro-survival pathway that plays an important role in the metabolic reprogramming of cancer cells. During cancer cell nutrient deprivation, the activity of mTOR is repressed, flipping the cells into a state in which intracellular resources are shunted away from anabolism and toward autophagy [42].

## Conclusions

Serum starvation of EOCs is a reliable way to induce their cellular dormancy *in vitro*. Moreover, stimulating the dormant cells with

5% serum allows them to resume their growth, which favors using this method in further experiments, for example those dedicated to identifying triggers and signaling pathways responsible for dormancy termination, reinitiation of EOC cell progression, and tumor relapse.

## Author contributions

Szymon Rutecki (Conceptualization [equal], Investigation [lead], Methodology [lead], Writing—original draft [lead]), Agnieszka Leśniewska-Bocianowska (Investigation [equal], Methodology [equal]), Klaudia Chmielewska (Investigation [equal], Methodology [equal]), Julia Matuszewska (Investigation [equal], Methodology [equal]), Eryk Naumowicz (Resources [equal]), Paweł Uruski (Investigation [equal]), Artur Radziemski (Investigation [equal]), Justyna Mikuła-Pietrasik (Conceptualization [equal], Investigation [lead], Methodology [lead]), Andrzej Tykarski (Resources [equal], Supervision [lead], Writing—review and editing [equal]), and Krzysztof Książek (Conceptualization [lead], Formal analysis [lead], Funding acquisition [lead], Project administration [lead], Resources [equal], Supervision [lead], Writing—review and editing [lead])

*Conflict of interest statement.* None declared.

## Funding

This study was supported by a grant from the National Science Centre, Poland (registration number 2020/37/B/NZ5/00100).

## Data Availability

Data supporting reported results can be provided by the corresponding author upon request.

## References

- Jelovac D, Armstrong DK. Recent progress in the diagnosis and treatment of ovarian cancer. *CA Cancer J Clin* 2011;**61**:183–203.
- International Collaborative Ovarian Neoplasm Group. Paclitaxel plus carboplatin versus standard chemotherapy with either single-agent carboplatin or cyclophosphamide, doxorubicin, and cisplatin in women with ovarian cancer: the ICON3 randomised trial. *Lancet* 2002;**360**:505–15.
- Giornelli GH. Management of relapsed ovarian cancer: a review. *Springerplus* 2016;**5**:1197.
- Kim S, Han Y, Kim SI *et al*. Tumor evolution and chemoresistance in ovarian cancer. *NPJ Precis Oncol* 2018;**2**:20.
- Chang JC. Cancer stem cells: role in tumor growth, recurrence, metastasis, and treatment resistance. *Medicine (Baltimore)* 2016;**95**:S20–S25.
- Sosa MS, Bragado P, Aguirre-Ghiso JA. Mechanisms of disseminated cancer cell dormancy: an awakening field. *Nat Rev Cancer* 2014;**14**:611–22.
- Shepherd TG, Dick FA. Principles of dormancy evident in high-grade serous ovarian cancer. *Cell Div* 2022;**17**:2.
- Santos-de-Frutos K, Djouder N. When dormancy fuels tumour relapse. *Commun Biol* 2021;**4**:747.
- Pradhan S, Sperduto JL, Farino CJ *et al*. Engineered *in vitro* models of tumor dormancy and reactivation. *J Biol Eng* 2018;**12**:37.

10. Triana-Martinez F, Loza MI et al. Beyond tumor suppression: senescence in cancer stemness and tumor dormancy. *Cells* 2020;**9**:346.
11. Aguirre-Ghiso JA. Models, mechanisms and clinical evidence for cancer dormancy. *Nat Rev Cancer* 2007;**7**:834–46.
12. Preciado J, Reátegui E, Azarin S et al. Immobilization platform to induce quiescence in dormancy-capable cancer cells. *Technology* 2017;**5**:129–38.
13. Lu Z, Luo RZ, Lu Y et al. The tumor suppressor gene ARHI regulates autophagy and tumor dormancy in human ovarian cancer cells. *J Clin Invest* 2008;**118**:3917–29.
14. Blessing AM, Santiago-O’Farrill JM, Mao W et al. Elimination of dormant, autophagic ovarian cancer cells and xenografts through enhanced sensitivity to anaplastic lymphoma kinase inhibition. *Cancer* 2020;**126**:3579–92.
15. Chawla K, Klein TJ, Schumacher BL et al. Tracking chondrocytes and assessing their proliferation with PKH26: effects on secretion of proteoglycan 4 (PRG4). *J Orthop Res* 2006;**24**:1499–508.
16. Sosińska P, Mikuła-Pietrasik J, Ryżek M et al. Specificity of cytochemical and fluorescence methods of senescence-associated beta-galactosidase detection for ageing driven by replication and time. *Biogerontology* 2014;**15**:407–13.
17. Damen MPF, van Rheenen J, Scheele C. Targeting dormant tumor cells to prevent cancer recurrence. *Febs J* 2021;**288**:6286–303.
18. Ponchio L, Duma L, Oliviero B et al. Mitomycin C as an alternative to irradiation to inhibit the feeder layer growth in long-term culture assays. *Cytotherapy* 2000;**2**:281–6.
19. Nagy JA, Chang SH, Dvorak AM et al. Why are tumour blood vessels abnormal and why is it important to know? *Br J Cancer* 2009;**100**:865–9.
20. Garcia-Jimenez C, Goding CR. Starvation and pseudo-starvation as drivers of cancer metastasis through translation reprogramming. *Cell Metab* 2019;**29**:254–67.
21. Yao G. Modelling mammalian cellular quiescence. *Interface Focus* 2014;**4**:20130074. <https://doi.org/10.1098/rsfs.2013.0074>
22. Domcke S, Sinha R, Levine DA et al. Evaluating cell lines as tumour models by comparison of genomic profiles. *Nat Commun* 2013;**4**:2126.
23. Beaufort CM, Helmijr JCA, Piskorz AM et al. Ovarian cancer cell line panel (OCCP): clinical importance of in vitro morphological subtypes. *PLoS One* 2014;**9**:e103988.
24. Alessio N, Aprile D, Cappabianca S et al. Different stages of quiescence, senescence, and cell stress identified by molecular algorithm based on the expression of Ki67, RPS6, and beta-galactosidase activity. *Int J Mol Sci* 2021;**22**:3102.
25. Demidenko ZN, Blagosklonny MV. Growth stimulation leads to cellular senescence when the cell cycle is blocked. *Cell Cycle* 2008;**7**:3355–61.
26. White EZ, Pennant NM, Carter JR et al. Serum deprivation initiates adaptation and survival to oxidative stress in prostate cancer cells. *Sci Rep* 2020;**10**:12505.
27. Park SY, Nam JS. The force awakens: metastatic dormant cancer cells. *Exp Mol Med* 2020;**52**:569–81.
28. Sun X, Kaufman PD. Ki-67: more than a proliferation marker. *Chromosoma* 2018;**127**:175–86.
29. Roche B, Arcangioli B, Martienssen R. Transcriptional reprogramming in cellular quiescence. *RNA Biol* 2017;**14**:843–53.
30. Gerdes J, Lemke H, Baisch H et al. Cell cycle analysis of a cell proliferation-associated human nuclear antigen defined by the monoclonal antibody Ki-67. *J Immunol* 1984;**133**:1710–5.
31. Higuchi A, Shimmura S, Takeuchi T et al. Elucidation of apoptosis induced by serum deprivation in cultured conjunctival epithelial cells. *Br J Ophthalmol* 2006;**90**:760–4.
32. Kobayashi A, Okuda H, Xing F et al. Bone morphogenetic protein 7 in dormancy and metastasis of prostate cancer stem-like cells in bone. *J Exp Med* 2011;**208**:2641–55.
33. Sharma S, Xing F, Liu Y et al. Secreted protein acidic and rich in cysteine (SPARC) mediates metastatic dormancy of prostate cancer in bone. *J Biol Chem* 2016;**291**:19351–63.
34. Roberson RS, Kussick SJ, Vallieres E et al. Escape from therapy-induced accelerated cellular senescence in p53-null lung cancer cells and in human lung cancers. *Cancer Res* 2005;**65**:2795–803.
35. Weaver VM, Petersen OW, Wang F et al. Reversion of the malignant phenotype of human breast cells in three-dimensional culture and in vivo by integrin blocking antibodies. *J Cell Biol* 1997;**137**:231–45.
36. Correa RJ, Peart T, Valdes YR et al. Modulation of AKT activity is associated with reversible dormancy in ascites-derived epithelial ovarian cancer spheroids. *Carcinogenesis* 2012;**33**:49–58.
37. Aguirre Ghiso JA, Kovalski K, Ossowski L. Tumor dormancy induced by downregulation of urokinase receptor in human carcinoma involves integrin and MAPK signaling. *J Cell Biol* 1999;**147**:89–104.
38. Aguirre-Ghiso JA, Estrada Y, Liu D et al. ERK(MAPK) activity as a determinant of tumor growth and dormancy; regulation by p38 (SAPK). *Cancer Res* 2003;**63**:1684–95.
39. Dhillon AS, Hagan S, Rath O et al. MAP kinase signalling pathways in cancer. *Oncogene* 2007;**26**:3279–90.
40. Zhang W, Liu HT. MAPK signal pathways in the regulation of cell proliferation in mammalian cells. *Cell Res* 2002;**12**:9–18.
41. Corazzari M, Gagliardi M, Fimia GM et al. Endoplasmic Reticulum Stress, Unfolded Protein Response, and Cancer Cell Fate. *Front Oncol* 2017;**7**:78.
42. Liu GY, Sabatini DM. mTOR at the nexus of nutrition, growth, ageing and disease. *Nat Rev Mol Cell Biol* 2020;**21**:183–203.